Journal of Applied Mechanics and Technical Physics, Vol. 41, No. 4, 2000

EFFECT OF FLOW NONPARALLELISM ON INSTABILITY OF THE TAYLOR–GÖRTLER WAVES IN SUPERSONIC AXISYMMETRIC JETS

N. M. Terekhova

UDC 532.526

Within the framework of the linear theory of hydrodynamic stability, the characteristics of the Taylor–Görtler waves are numerically simulated at the initial section of a supersonic axisymmetric jet taking into account the effects of flow nonparallelism and expansion. The special features of the streamwise dynamics of the growth rates of various wave components for turbulent, weakly nonisobaric, and laminar jets are studied. It is shown that the growth rates depend strongly on the quantity on which their determination is based, the position of the point where it is measured, and the flow regime. Some experimental results are discussed, and a method for determining the growth rates is proposed.

Introduction. The objective of the present work is to study the effect of nonparallelism of the mean flow fields, which is related to expansion of a supersonic axisymmetric jet, on the characteristics of disturbances of rotational or centrifugal instability — Taylor–Görtler waves. In nonisobaric jets, these waves have the form of a system of streamwise quasi-stationary vortices enclosed in the mixing layer of the initial section. This type of instability in jets is of great interest, which is evidenced by the large number of experimental works [1–6]. Most works note the existence of transverse-azimuthal overflow of the gas mass, which leads to significant deviations of the parameters from their mean values. Variations of the excess total pressure in streamwise sections, which allow one to obtain data on the streamwise dynamics of waves, were measured only in [4–6].

Results of systematic numerical and theoretical studies of the characteristics and structure of such disturbances are described in [5, 7–10]. It is shown in [7] that quasi-stationary waves may occur in nonisobaric jets if we take into account centrifugal forces arising in the motion along curved trajectories of the initial section. It was found in [5, 8] that both the wave growth rates and the transverse-azimuthal developments of the wave fields can be described in the plane-parallel approximation with ignored viscosity. The structures of streamwise vortices are studied in detail in [9], and their basic dependences on some governing parameters are established.

Studying the problem with consideration of viscosity [10] allowed one to determine the ranges of existence of an unstable process and the critical Reynolds numbers of the loss of stability and to propose some criterial estimates. It is also shown that, at low Reynolds numbers, the wave spectrum consists of only one prevailing, maximally unstable mode. An increase in the Reynolds number leads to the expansion of the spectral composition and, hence, to the complication of the structure of wave fields and wave configurations.

Some aspects remain unstudied, and without examining them, the analysis cannot be considered to be complete, since some properties of the disturbances observed are not described by the theory. Rapid destruction of high-mode components is observed in the experiment upon jet spreading, whereas the inviscid calculations show that the growth rates of small-scale components gradually increase with increasing mode

Institute of Theoretical and Applied Mechanics, Siberian Division, Russian Academy of Sciences, Novosibirsk 630090. Translated from Prikladnaya Mekhanika i Tekhnicheskaya Fizika, Vol. 41, No. 4, pp. 33–41, July–August, 2000. Original article submitted May 13, 1999; revision submitted July 1999.

 0021-8944/00/4104-0604 $25.00

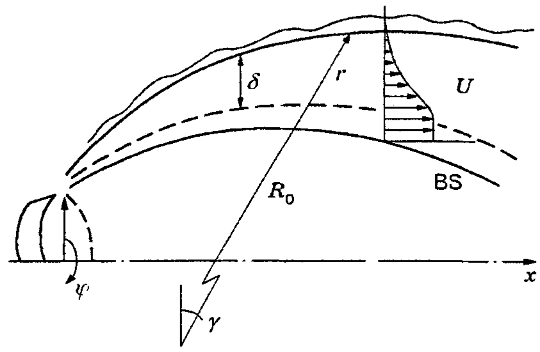

Fig. 1

number, and, according to the theory, these components should increase more rapidly. At the same time, the growth rates of the waves of small azimuthal modes registered in experiments as the dominating ones are lower than their theoretical values. It was also noted [4, 5] that there are large-scale disturbances (with small azimuthal wavenumbers) in the near-root regions, which decay downstream.

The difference between the experimental and theoretical data may be caused both by experimental errors (the accuracy is not very high) and by the fact that the theory does not take into account a number of factors (for example, the mean-velocity nonparallelism at the initial section and the dependence of the mean and wave characteristics on the streamwise coordinate).

The objective of the present work is to study the effect of nonparallelism and downstream expansion of the jet on wave stability. Viscosity was ignored in these studies, since the experiments were conducted for Reynolds numbers $\mathrm{Re} \approx 10^7$ for which viscosity exerts a minor effect.

Governing Equations and Methods of Solution. The flow scheme at the initial section of an underexpanded jet is shown in Fig. 1. We consider a compressed layer of the first barrel of an axisymmetric ambient nonisobaric jet whose transverse length is from the external boundary of the barrel shock (BS) to the mixing-layer boundary and whose streamwise length is from the nearest boundary of the nozzle exit to the Mach disk. The shocks and changes in the mean parameters in these shocks are not considered, but it is assumed that the BS position determines the values of the curvature radii R_0 and, hence, the centrifugal force proportional to U^2/R_0. In the streamwise direction, the length of the computational domain is expressed through the mixing-layer thickness δ. The range under consideration $0.1 < \delta < 0.65$ corresponds to the actual dimensionless thickness of the mixing layer.

We used the curvilinear orthogonal coordinates $R = R_0 + r$, where r is the radial variable and R_0 is the curvature radius ($R_0 \gg r$), and the angular variables φ and γ, which are the azimuthal and longitudinal angles, respectively (Fig. 1). They correspond to the radial, azimuthal, and longitudinal components of velocity v, w, and u. If $R_0 = \mathrm{const}$, the streamwise coordinate x may be introduced by the relation $dx = R_0 d\gamma$. Zheltukhin and Terekhova [7] derived the complete inviscid system of equations in these coordinates:

$$v_t + vv_r + wv_\varphi/r + uv_x - w^2/r - u^2/R = -p_r/\rho,$$

$$w_t + vw_r + ww_\varphi/r + uw_x + vw/r = -p_\varphi/\rho r, \quad u_t + vu_r + wu_\varphi/r + uu_x = -p_x/\rho, \tag{1}$$

$$\rho_t + v\rho_r + w\rho_\varphi/r + u\rho_x + \rho(v_r + w_\varphi/r + u_x + v/r) = 0,$$

$$S_t + vS_r + wS_\varphi/r + uS_x = 0, \qquad S = \ln\,(p/\rho^k)^{c_v}.$$

Here p is the pressure, ρ is the density, and S is the entropy. System (1) is written for dimensional quantities, and the method of normalization is described below. In (1), only the main centrifugal term in the equation for v is taken into account. As is shown in [7], the effect of the Coriolis force vu/R in the equation for u

and the geometric effect $\rho v/R$ in the continuity equation is negligibly small. An ambient cold air jet with $k = c_P/c_V = 1.4$ is considered.

In our analysis with nonparallelism effects taken into account, we used the results of [11, 12]. We assume that the mean flow weakly depends on the coordinate in the streamwise direction. We introduce a slow variable $s = \chi x$, where the small parameter χ characterizes the degree of jet expansion. The velocity field, density, and pressure are represented in the form $\bar{u} = [\varepsilon V(r,s) + \varepsilon v', \varepsilon w', U(r,s) + \varepsilon u']$, $\varrho(r,s) + \varepsilon\rho'$, and $P(r) + \varepsilon p'$. The dependence of the mixing-layer thickness δ on the coordinate x determines the so-called streamwise bindings $\delta(x)$ or $\chi = d\delta/dx$ related to the flow character or regime.

For jets with moderate pressure ratios, the realistic range of dimensionless curvature radii seems to be $5 < R_0 < 25$, which was studied in the present paper.

It is assumed that the compressed layer consists of two subregions. In the first, "inviscid" one [13], which extends from the external boundary of the BS to the line of the maximum excess total pressure (the dashed curve in Fig. 1), the total pressure is recovered, the mean velocity increases (to a maximum value), and the flow parameters are determined from the perfect-gas equations. In the second subregion (mixing layer), there is a smooth transition from the parameters at the internal boundary of the compressed layer to the parameters of the ambient space.

The streamwise velocity and density in the first subregion are assumed to be constant and equal to their maximum values. In averaging Eqs. (1), the values of the mean velocity $\bar{U}$ and mean density $\bar{\varrho}$ in this analog of the potential core are assumed to have characteristic values.

The dimensionless profiles of the mean velocity in mixing layers are defined by the following expression:

$$U(r) = \exp(-0.693\eta^2), \quad \eta = 2(r - r_1)/\delta, \quad r_1 = 1 - \delta/2. \tag{2}$$

This approximation formula satisfactorily describes the actual distributions [11, 14].

The characteristic dimensional linear scale is chosen as $\bar{r}$ for which the dimensional velocity is half of the characteristic value; therefore, we have $U = 0.5$ for $r = 1$ in the dimensionless form. The value $r = 1$ coincides with half of the thickness of the mixing layer whose length is $r_1 < r < 1 + \delta/2$.

The mean density ϱ is related to U as $\varrho = [1 + (k-1)\mathrm{M}_0^2(1 - U^2)/2]^{-1}$, and the velocity of sound is determined from the equation $a^2 = [\varrho \mathrm{M}_0^2]^{-1}$. The value of the Mach number M_0 entering into the main equations is also determined from the line of the maximum velocity. Using isentropic relations, it can be related to the Mach number at the nozzle exit M_a.

We seek wave solutions slowly changing along the streamwise coordinate (only the pressure component is written here) in the form

$$p'(r,\varphi,x,t) = p(r,s)\exp(i\tau + in\varphi), \quad \tau = \Theta(x) - \omega t, \tag{3}$$

where $d\Theta/dx = \alpha(s)$ ($\alpha = \alpha^r + i\alpha^i$). Here α^r and n are the streamwise and azimuthal wavenumbers, α^i is the amplification factor in the streamwise direction, and the angular frequency ω is real. For the Taylor–Görtler waves, we have $(p', v', u', \rho') = (p(r,s), v(r,s), u(r,s), \rho(r,s))\exp(i\tau)\cos(n\varphi)$ and $w' = iw(r,s)\exp(i\tau)\sin(n\varphi)$. The value of n determines the number of vortices or vortex pairs on the jet circumference. Small and large values of n correspond to large-scale and small-scale vortices, respectively.

For the Taylor–Görtler vortices, α^r and ω are equal to zero. To avoid singularities during integration of (1) for $U \to 0$, the calculations were performed for small frequencies other than zero defined by the acoustic Strouhal number $\mathrm{Sh} = 2\pi\bar{\omega}\bar{r}/\bar{a}$, where $\bar{a}$ is the velocity of sound outside the mixing layer. It was generally accepted that $\mathrm{Sh} = 0.005$, and small values of α^r other than zero were obtained.

The complex amplitude functions of disturbances can be expanded into the asymptotic series

$$p(r,s) = \sum_j \varepsilon^j p_j(r,s). \tag{4}$$

We confine ourselves to two terms of expansion. Linearizing (1) in terms of ε for waves (3) and (4), we obtain the system

$$iFv_j + p_j'/\varrho - 2Uu_j/R = -\varepsilon^j B_1, \qquad iFw_j + inp_j/(\varrho r) = -\varepsilon^j B_2,$$

$$iFu_j + U'v_j + i\alpha p_j/\varrho = -\varepsilon^j B_3, \tag{5}$$

$$iF\mathrm{M}_0^2 p_j + v_j' + v_j/r + inw_j/r + i\alpha u_j = -\varepsilon^j B_4, \quad F = \alpha U - \omega, \quad j = 0, 1,$$

with the boundary conditions $p_j \to 0$ for $r \to 0$ and $r \to \infty$. Hereinafter, the prime denotes the derivative with respect to r. The amplitude functions of the wave components and the boundary conditions on them can be expressed through the amplitude function of the pressure p.

It is more convenient to solve system (5) for the function p. The reduced equation for $j = 0$ corresponding to the plane–parallel approximation has the form

$$L(p_0) \equiv p_0'' + G_1 p_0' + G_2 p_0 = 0, \tag{6}$$

where $G_1 = G_1^0 + G_1^R$, $G_2 = G_2^0 + G_2^R$, $G_1^0 = 1/r - \varrho'/\varrho - 2F'/F$, and $G_2^0 = F^2/a^2 - n^2/r^2 - \alpha^2$; the additional terms $G_1^R = 2\alpha U/(FR) - 2F'B/(FE) + B'/E$ and $G_2^R = B(n^2/(rF)^2 - 1/a^2) + 2(F' - \alpha U(\varrho'/\varrho + 2F'(1 + B/E)/F - B'/E - 1/r))/(FR)$ $(B = 2UU'/R,\ E = F^2 - B)$ are determined by the presence of the centrifugal force.

The boundary conditions in regions of constant mean parameters are expressed through the modified Bessel functions

$$\begin{aligned} p_0 &= C_1 I_n(\lambda_1 r), \qquad p_0' = C_1 I_n'(\lambda_1 r), \qquad r \to 0, \\ p_0 &= C_2 K_n(\lambda_2 r), \qquad p_0' = C_2 K_n'(\lambda_2 r), \qquad r \to \infty, \qquad \lambda^2 = F^2/a^2 - \alpha^2. \end{aligned} \tag{7}$$

The formulated boundary-value problem for eigenvalues allows us to determine the eigenvalue of α in the plane–parallel approximation.

The corresponding eigenfunction p_0 has an arbitrary amplitude $A(s)$: $p_0 = A(s)P_0(r, s)$. For P_0, the same equation as for p_0 is valid [Eq. (6) with boundary conditions (7)], and the wave solution of zero order is written in the form

$$p(r, \varphi, x, t) = A(s)P_0(r, s) \exp(i\tau) \cos(n\varphi) + O(\varepsilon). \tag{8}$$

For the first-order approximation in terms of ε $(j = 1)$, system (5) yields a system of inhomogeneous equations whose right sides contain the functions of zero order, their derivatives with respect to r and x, the mean transverse velocity V determined from the continuity equation, and the mean-velocity gradients:

$$B_1 = V'v_0 + Vv_0' + Uv_{0x}, \qquad B_2 = Vw_0/r + Vw_0' + Uw_{0x},$$

$$B_3 = U_x u_0 + Vu_0' + Uu_{0x} + p_{0x}/\varrho, \qquad B_4 = (V' + V/r + U_x)p_0 + Vp_0'/a^2 + Up_{0x}/a^2 + \varrho u_{0x}.$$

Here $p_0 = AP_0$, $p_{0x} = AP_{0x} + P_0 A_x$, $v_0 = AV_0$, $v_{0x} = AV_{0x} + V_0 A_x$, $w_0 = AW_0$, $w_{0x} = AW_{0x} + W_0 A_x$, $u_0 = AU_0$, $u_{0x} = AU_{0x} + U_0 A_x$, P_0 is the solution of (6), and V_0, W_0, and U_0 are expressed in terms of P_0 from (5).

Reducing the inhomogeneous system to one equation for p_1

$$L(p_1) = N_1 A + N_2 \frac{dA}{dx},$$

where $N \equiv N_1 + N_2 = i(D_1' + inD_2/r + i\alpha D_3 + D_1/r + B_4/\varrho)\varrho E/F$, $D_1 = (iFB_1 + 2UB_3/R)/E$, $D_2 = iB_2/F$, and $D_3 = (iFB_3 - U'B_1)/E$, we can easily see that the operator $L(p_1)$ is equivalent to operator (6). The operator $L(p_1)$ is degenerate; therefore, a solution for p_1 exists under the condition of orthogonality of the right side of the equation to the solution of the Π problem conjugate to (6) and (7):

$$\int_r \Big(N_1 A + N_2 \frac{dA}{dx}\Big)\Pi\, dr = 0. \tag{9}$$

The equation for Π is easily obtained from (6):

$$\Pi'' - (G_1\Pi)' + G_2\Pi = 0.$$

The boundary conditions are found from the bilinear form $\Psi[p_0\Pi] = p_0\Pi/r + p_0'\Pi - p_0\Pi'$ and conditions (7).

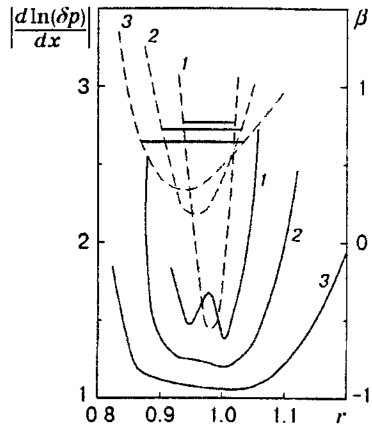

Fig. 2

The coefficient of streamwise amplification of zero-order disturbances β for a weakly nonparallel flow is determined from (8):

$$\beta \equiv \text{Real}\,\frac{d\ln p}{dx} = \text{Real}\Big(i\alpha + \frac{d\ln A}{dx} + \frac{d\ln P_0}{dx}\Big). \tag{10}$$

Using the condition of solubility of Eq. (9), we can express the logarithmic derivative $A(x)$:

$$\frac{d\ln A}{dx} = -\int\limits_r N_1\Pi\,dr \Big/ \int\limits_r N_2\Pi\,dr.$$

The gradients in Eq. (10) depend on the value of χ, which can vary in a wide range depending on the flow regime and jet pressure ratio. It is much greater for a turbulent jet than for a laminar one because of enhanced mixing, and it is greater for an underexpanded jet with high pressure ratios than for a weakly nonisobaric jet.

In free jet flows (in contrast to the near-wall boundary layers), the distribution of the mean velocities in mixing layers is independent of the flow regime, and relation (2) is valid for the laminar, transitional, and turbulent jets. This was shown theoretically for planar jets [15] and noted many times in experiments with axisymmetric jets (see [14]). Hence, the transverse gradients of the mean and wavy components are identical. The change in the thickness of free boundary layers is determined by the state of the flow and exhaustion regime; hence, the derivatives with respect to the streamwise coordinate may vary within wide limits.

In this paper, we consider three regimes of air jet exhaustion for $M_0 = 1.5$:

(1) turbulent jet with a large pressure ratio ($\chi_1 = 0.2281$ [16]);

(2) turbulent, weakly underexpanded jet ($\chi_2 = 0.157$ [6]);

(3) laminar isobaric jet ($\chi_3 = 0.08732$ [11]).

In this case, we have $\delta = \chi x + \delta_0$, where δ_0 is the initial thickness of the mixing layer for $x = 0$. The latter regime allows us to evaluate the influence of the exhaustion regime on χ. The flow parameters of the third regime are close to the flow parameters with weak nonisobaricity.

The values of χ in each regime differ by several times. The degree of expansion depends on the composition of the jet and the medium whereto the exhaustion is performed.

Results and Discussion. The experiments [17] show that the growth rates in a subsonic boundary layer depend on the quantity from which they are determined and on the transverse coordinate in which this quantity is measured. This is confirmed by numerical and theoretical studies in a supersonic boundary layer [12]. To establish these dependences in the jet, the streamwise dynamics of several parameters was studied: the pressure perturbations determined by Eq. (6), density perturbations, and total pressure perturbations (or variations) [4–6].

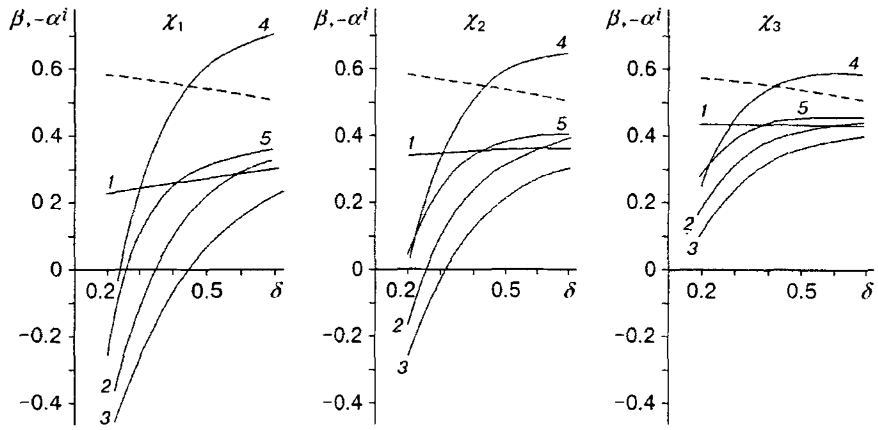

Fig. 3

Variations of the total pressure δp are constructed using the known gas-dynamic relation from which, with accuracy to quadratic terms, we obtain the expression $\delta p = p/P + k\mathrm{M}^2((1-k)p/(kP) + 2u/U)/(2 + (k-1)\mathrm{M}^2)$, where M is the local Mach number [7-9].

It follows from the results plotted in Fig. 2 that the position of the measured quantity along the transverse coordinate significantly affects the growth rate. For exhaustion regime 2, Fig. 2 shows the calculation results for the mode $n = 16$ for $R_0 = 20$ and the mixing-layer thickness $\delta = 0.15$, 0.30, and 0.45 (curves 1–3). The solid curves show the distributions of the absolute value of the logarithmic derivative $|d \ln(\delta p)/dx|$. It is seen that this quantity, which enters Eq. (10), changes significantly in the mixing layer. Hence, the coefficient β also depends strongly on r (dashed curves in Fig. 2). The straight lines show the values of $-\alpha^i$ for the plane-parallel approximation.

For moderate values of the thickness (for example, $\delta = 0.15$), there exists even a range of negative values of β, where the disturbances are decaying. The presence of these "tongues" is related to the reconstruction of wave configurations [9], where a vortex existing at a small thickness δ is displaced from the mixing layer by a counterrotating vortex. For large δ, there are no negative values of β, but the strong dependence on the transverse variable is retained. Hence, in measuring the growth rates, one has to determine exactly the location of the measured quantities. We consider this problem in more detail. The values of β were calculated for three exhaustion regimes from different quantities (Fig. 3): from the amplitude function of pressure in its maximum (6) (curve 1), from the amplitude function of density in its maximum (curve 2), from variation of the total pressure δp in its maximum (curve 3), from δp at the line of the halved averaged total pressure (curve 4), and from δp at the line of the halved mean velocity $U = 0.5$ (curve 5). Curves 1–3 are of purely theoretical interest, since the experiments register a rather complicated multimode spectrum of disturbances [4, 5, 8], and it is difficult to determine the coordinates of the first three quantities in experiment. The last two quantities can serve as bindings in measurements, and the coordinate of the latter can be easily determined since it coincides with the half-width of the mixing layer.

The dashed curves in Fig. 3 show the growth rates $-\alpha^i$ in the plane-parallel approximation. The maximum difference between the curves for $-\alpha^i$ and β (solid curves) is observed for small δ (in the near-root region). With increasing δ, these curves come closer. It is also seen that the growth rates of disturbances in regime 1 are significantly lower for a turbulent jet than for a laminar one (regime 3), which is related to enhanced mixing.

It was found that the increments significantly depend on the quantities from which they are determined. Generally, the values of β are lower than the corresponding values of $-\alpha^i$. This is in qualitative agreement with the experiments of [5, 8]. This regularity is invalid for curve 4. It has a strong longitudinal gradient; therefore, large errors are possible in determining β. For small δ, disturbances in turbulent regimes may be

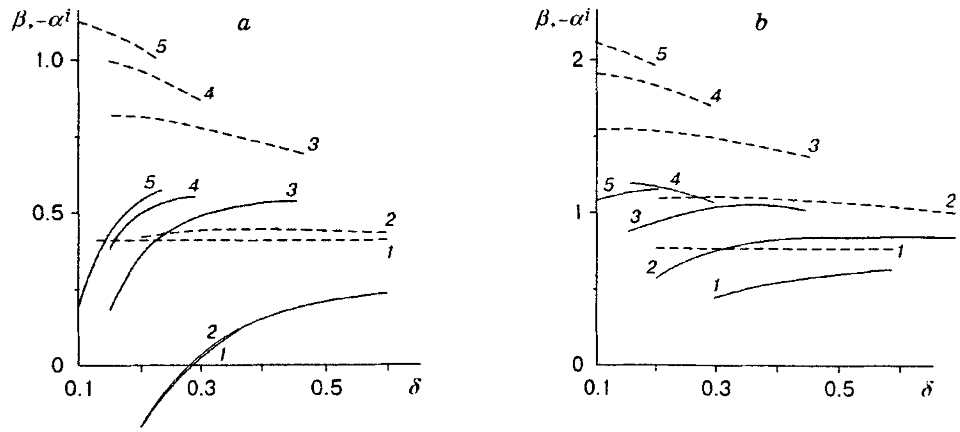

Fig. 4

decaying ($\beta < 0$), whereas the theoretical values of $-\alpha^i$ are always positive.

Similar features are typical of jets with a significant curvature of the boundaries (small R_0). With increasing centrifugal forces, the growth rates of disturbances increase significantly; the flow expansion in the near-root regions leads to a decrease in β as compared to the plane-parallel approximation but does not involve the decay of waves with small azimuthal numbers.

Since the problem is multiparametric, it is difficult to find a suitable form for representation of the res[illegible] We chose regime 2 (χ_2) for δp (curve 5 in Fig. 3). These dependences of the growth rates $\beta(\delta)$ for a number of modes are plotted in Fig. 4a and b for $R_0 = 20$ and 5, respectively. The dashed curves show the growth rates $-\alpha^i$ for modes $n = 4$, 8, 16, 24, and 30 (curves 1–5). The solid curves show β with jet expansion taken into account for the same values of n. The difference in the growth rates is particularly well seen in t[illegible]gion of small δ. This difference increases with increasing azimuthal wavenumber. We also note that the growth rates β do not decrease (as $-\alpha^i$) but increase with increasing mixing layer.

Only a qualitative comparison with experimental data is possible at the moment. Taking into account the nonparallelism offers an explanation as to some special features observed in the experiment, for example, the decay of moderate azimuthal components in the near-root region and the lower growth rates than those predicted by the plane–parallel approximation [4, 5, 8].

The calculation results show that the growth rates of the Taylor–Görtler waves in expanding supersonic jets depend significantly on the transverse coordinate. Therefore, it is important in the experiment to determine exactly the coordinates of the point where the corresponding quantity is measured.

REFERENCES

1. S. A. Novopashin and A. L. Perepelkin, "Self-organization of flow in a supersonic preturbulent jet," Preprint No. 175-88, Inst. of Thermal Physics, Novosibirsk (1988).
2. A. Krothopalli, G. Buzuna, and L. Lourenco, "Streamwise vortices in an underexpanded axisymmetric jet," *Phys. Fluids A*, **3**, No. 8, 1848–1851 (1991).
3. F. P. Welsh and T. M. Cain, "Electron beam visualization of low density nitrogen plumes," in: Proc. of the 7th Symp. of the Flow Visual., Seattle (1995), pp. 192–197.
4. V. I. Zapryagaev, S. G. Mironov, and A. V. Solotchin, "Spectral composition of wavenumbers of longitudinal vortices and characteristics of the flow structure in a supersonic jet," *Prikl. Mekh. Tekh. Fiz.*, **34**, No. 5, 41–47 (1993).
5. N. A. Zheltukhin, V. I. Zapryagaev, A. V. Solotchin, and N. M. Terekhova, "Spectral composition and structure of stationary Taylor–Görtler vortices in a supersonic jet," *Dokl. Akad. Nauk SSSR*, **325**, No. 6, 1133–1137 (1992).

6. V. I. Zapryagaev, "The complex investigation method of 3-D disturbances at a curved shear layer of the nonisobaric supersonic jet," in: *Proc. of the 9th Int. Conf. of the Methods of Aerophys. Res.*, Part 3, Novosibirsk (1998), pp. 295–300.
7. N. A. Zheltukhin and N. M. Terekhova, "Disturbances of high modes in a supersonic jet," *Prikl. Mekh. Tekh. Fiz.*, No. 2, 75–82 (1990).
8. N. A. Zheltukhin and N. M. Terekhova, "Taylor–Görtler instability in a supersonic jet," *Prikl. Mekh. Tekh. Fiz.*, **34**, No. 5, 48–55 (1993).
9. N. M. Terekhova, "Streamwise vortices in axisymmetric jets," *Prikl. Mekh. Tekh. Fiz.*, 37, No. 3, 45–57 (1996).
10. N. M. Terekhova, "Viscous Taylor–Görtler instability in a supersonic axisymmetric jet," *Teplofiz. Aéromekh.*, **6**, No. 3, 307–318 (1999).
11. P. J. Morris and C. K. W. Tam, "Near and far fields noise from large-scale instability of axisymmetric jets," AIAA Paper No. 77-1351 (1977).
12. S. A. Gaponov and A. A. Maslov, *Evolution of Disturbances in Compressible Flows* [in Russian], Nauka, Novosibirsk (1980).
13. V. G. Dulov and G. A. Luk'yanov, *Gas-Dynamics of Exhaustion Processes* [in Russian], Nauka, Novosibirsk (1984).
14. V. N. Glaznev, "Self-induced oscillations with acoustic feedback upon exhaustion of supersonic off-design jets," Doct. Dissertation in Phys.-Math. Sci., Novosibirsk (1991).
15. H. Schlichting, *Boundary Layer Theory*, McGraw-Hill, New York (1968).
16. G. N. Abramovich (ed.), *Theory of Turbulent Jets* [in Russian], Nauka, Moscow (1984).
17. Y. S. Kachanov and T. G. Obolensteva, "A method of study of the influence of flow nonparallelism on the 3d stability of the Blasius boundary layer," in: *Proc. of the 8th Int. Conf. of the Methods of Aérophys. Res.*, Part 2, Novosibirsk (1996), pp. 100–105.